

Photochemistry of metal nitrosyl complexes. Delivery of nitric oxide to biological targets

P.C. Ford *, J. Bourassa, K. Miranda, B. Lee, I. Lorkovic, S. Boggs,
S. Kudo, L. Laverman

Department of Chemistry, University of California, Santa Barbara, CA 93106, USA

Received 28 July 1997; accepted 19 November 1997

Contents

Abstract	185
1. Introduction	186
2. NO detection in photoreaction solutions	186
3. Iron sulfur nitrosyl clusters (Roussin's anions)	187
3.1. Reactions of $\text{Fe}_4\text{S}_3(\text{NO})_7^-$ and $\text{Fe}_4\text{S}_3(\text{NO})_8^{2-}$ under continuous photolysis	189
3.2. Flash photolysis investigations of RBS and RRS	193
3.3. Radiation sensitization using RRS	194
3.4. Roussin's red "esters"	195
4. Activation parameters for the reactions of NO with Ferri-Hemes	195
5. Flash photolysis of $\text{Ru}(\text{TPP})(\text{ONO})(\text{NO})$	199
6. Summary	201
Acknowledgements	201
References	202

Abstract

The discoveries that nitric oxide serves important roles in mammalian bioregulation and immunology have stimulated intense interest in the chemistry and biochemistry of NO and derivatives such as metal nitrosyl complexes. Also of interest are strategies to deliver NO to biological targets on demand. One such strategy would be to employ a precursor which displays relatively low thermal reactivity but is photochemically active to give NO. This proposition led the authors to investigate photochemical properties of metal nitrosyl complexes such as the iron-sulfur-nitrosyl Roussin cluster anions $\text{Fe}_2\text{S}_2(\text{NO})_4^{2-}$ and $\text{Fe}_4\text{S}_3(\text{NO})_7^-$ as well as metalloporphyrin nitrosyls including ferriheme complexes (with M. Hoshino of the Institute of Physical and Chemical Research, Japan) and nitrosyl nitrito complexes of ruthenium porphyrins $\text{Ru}(\text{P})(\text{ONO})(\text{NO})$. Continuous and flash photolysis studies of these com-

* Corresponding author. Fax: +1 805 893 41 20.

pounds are reviewed here as are studies (with D.A. Wink and J.B. Mitchell of the Radiation Biology Branch of the US National Cancer Institute) using metal nitrosyl photochemistry as a vehicle for delivering NO to hypoxic cell cultures in order to sensitize γ -radiation damage. © 1998 Elsevier Science S.A.

Keywords: Nitric oxide; Photochemistry; Nitrosyl; Roussin's salts; Ruthenium; Iron; Porphyrins

1. Introduction

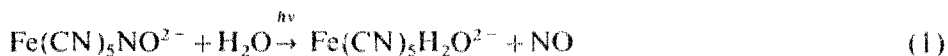
Nitric oxide is a molecule of considerable biological and biochemical interest, having been shown in recent years to play multiple roles in mammalian physiology, for example, as a bioregulatory agent in vasodilation and neural signaling and as a weapon of macrophages in immune response to pathogen invasion [1,2]. Such interest extends to coordination chemists as well, since much of the biochemistry of NO involves metal nitrosyl complexes. Metal nitrosyls can also be seen as useful delivery agents of nitric oxide and, in particular, hold promise for the photochemical delivery of NO to biological targets. Photochemical delivery from thermally stable compounds would allow for specific targeting through control of irradiation areas and intensities. It should be emphasized that there is a rich history of nitrosyl complex photochemistry, especially that involving metalloporphyrins (see for example refs. [3–12]). Since light transmission of mammalian tissues is more effective at longer wavelengths, complexes photosensitive to red light are of special interest.

In this context, a growing research effort at UC Santa Barbara has been concerned with quantitative investigations of various compounds which may serve as photochemical precursors of NO to desired targets *in vitro* and, eventually, *in vivo* on demand. These have employed both continuous and flash photolysis studies of known and new compounds. It was also necessary to refine electrochemical methods for nitric oxide detection in solution in order to evaluate quantitatively the photochemical release of NO. In addition, collaborative efforts with researchers at the US National Cancer Institute were necessary in order to evaluate biological effects of certain photoactive NO precursors. An overview of several ongoing studies along these lines is presented here.

2. NO detection in photoreaction solutions

A key problem in studying the photochemistry of metal nitrosyls is identifying and quantifying the NO released as a product since free NO does not have a distinctive spectroscopic signature in solution. For example, the photochemistry of sodium nitroprusside (a vasodilator used in hypertensive emergencies) has been studied repeatedly, but only recently was the NO release quantified by trapping with a nitronyl nitroxide to give an ESR active species [13]. Since this technique has the undesirable requirement of another chemically active species added to the photolysis

solution, we undertook to extend recently reported NO specific electrode technology [14,15] to such quantitative measurements. This involved characterizing and evaluating quantitative behavior of various custom designed electrode sensors, including one based on a mechanical pencil lead, as well as a newly available commercial electrode [16]. The key to accurate use of these electrodes is internal standardization directly in the photolysis medium with reliable solutions of known [NO]. By using both the commercial and custom electrodes, it was demonstrated quantitatively that the stoichiometry of nitroprusside photodecomposition is 0.95 ± 0.03 , i.e.



The experiment is illustrated in Fig. 1: the slow decay of the NO electrochemical signals can be attributed to NO autoxidation in these aerated solutions [17].

3. Iron sulfur nitrosyl clusters (Roussin's anions)

Although the anions of Roussin's black salt, $\text{Fe}_4\text{S}_3(\text{NO})_7^-$ (RBS), and of Roussin's red salt, $\text{Fe}_2\text{S}_2(\text{NO})_4^{2-}$ (RRS), were first described in the mid-19th century [18], their photochemistry has only recently drawn attention.

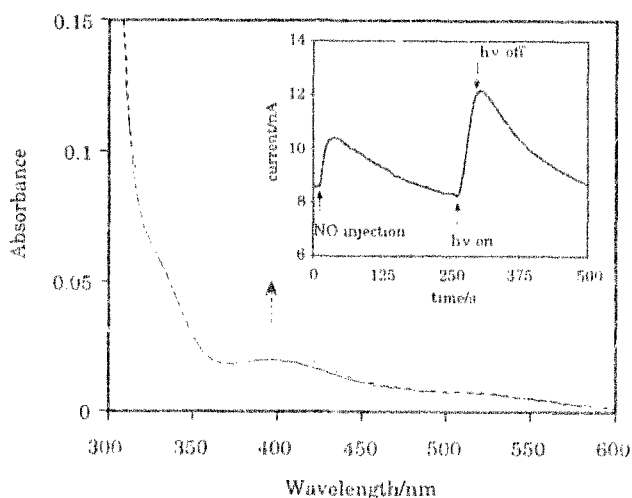
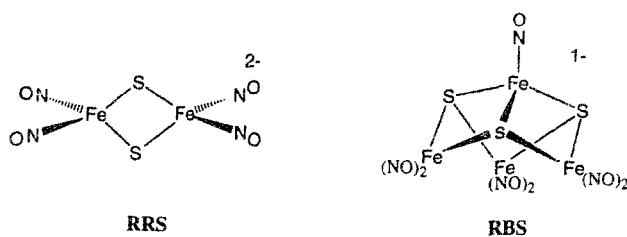


Fig. 1. Chronoamperogram of NO released by photolysis of 1 mM sodium nitroprusside in aerated pH 7.0 phosphate buffer solution (0.1 M) using broadband irradiation (360–440 nm). The NO sensor was a custom designed combination electrode calibrated immediately before photolysis by injecting standardized NO solution to give $8.85 \mu\text{M}$ [NO]. Photolysis for 28 s gave a signal for NO corresponding to $\Delta[\text{NO}] = 18.5 \mu\text{M}$, while the absorption change at 394 nm (0.014) corresponds to a $\Delta[\text{Fe}(\text{CN})_5\text{NO}^{2-}] = 19.6 \mu\text{M}$, a stoichiometric ratio of 0.94 for this experiment. The slow decay of the electrochemical signal is the result of NO autoxidation under these conditions.



The water soluble Roussin's salts were chosen for our studies not only because they carry numerous NO equivalents, but also because their optical spectra have absorptivities (Fig. 2) into the red, a feature attractive for possible use in tissues. The RBS

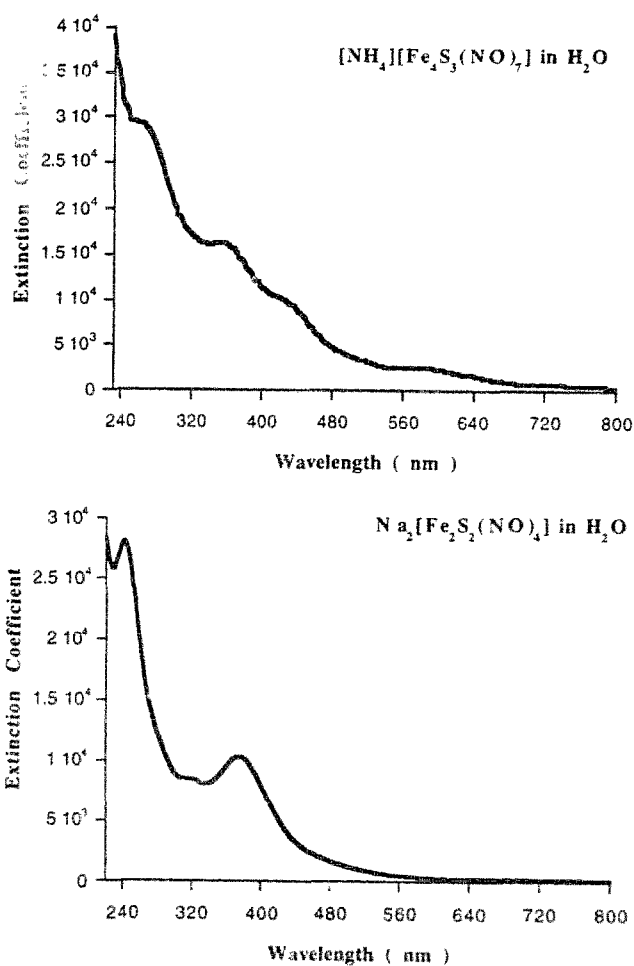


Fig. 2. Spectra of aqueous solutions of RBS and RRS.

anion has been the subject of several studies with vascular and brain tissues as a drug for the thermochemical or photochemical delivery of NO [19,20]; indeed, a biological assay (rat tail artery relaxation) was used to demonstrate the NO release from RBS upon photolysis in buffer solutions [19]. The red salt anion RRS has primarily been studied as a synthetic precursor; for example, it reacts with haloalkanes to form red “esters”, $\text{Fe}_2(\text{SR})_2(\text{NO})_4$ [21]. The quantitative photochemistry of neither the anions nor the esters had received attention until we initiated the present study [22].

As their names imply, the Roussin's red and black salts are highly colored compounds with strong absorptions in the visible (Fig. 2). The observable bands are broad and overlap considerably, possessing moderately high extinction coefficients (10^3 – $3 \times 10^3 \text{ M}^{-1} \text{ cm}^{-1}$) that suggest charge transfer character. The RBS broad, lowest energy absorption band at 580 nm extends further into the red, although extinction coefficients are only in the range of $10^3 \text{ M}^{-1} \text{ cm}^{-1}$. The red Roussinate anion's strongest transition at 374 nm tails far into the visible, but it has no distinctive bands at longer wavelengths. There is clearly a need for understanding better the photoactive excited states of these iron sulfur nitrosyl clusters, especially the lowest energy excited states (LEES), since the independence of quantum yields to the irradiation wavelength (λ_{irr}) would be consistent with the cascade of initially formed states to a common LEES (see below). Extended Hückel molecular orbital calculations suggest that the ground state LUMO has Fe–Fe and Fe–S and Fe–NO some antibonding character [23,24]. Hence excitation might be expected to lead to cluster fragmentation. However, it was pointed out to us (private comment from L. Noodleman) that in analogy to other iron sulfur clusters [25], the Fe centers are likely to be antiferromagnetic coupled high spin Fe^{3+} and/or Fe^{2+} (which EHMO theory does not treat) with the nitrosyls (formally) negatively charged. In such a case the LEES may be NO-to-iron charge transfer states with enhanced lability of the Fe–NO bonds.

3.1. Reactions of $\text{Fe}_4\text{S}_3(\text{NO})_7^-$ and $\text{Fe}_2\text{S}_2(\text{NO})_4^{2-}$ under continuous photolysis

Roussin's black salt is thermally stable over the course of many hours in aerated aqueous solutions. Photolysis of such solutions leads to optical density decreases broadly across the visible spectrum (Fig. 3). Table 1 summarizes the quantum yields for RBS disappearance (Φ_d) for a variety of irradiation wavelengths (λ_{irr}). These showed little dependence on λ_{irr} , giving an average Φ_d value of $\sim 10^{-3}$ from $\lambda_{\text{irr}} = 313$ to 546 nm in aerated aqueous solutions [22]. However, in deoxygenated solutions, RBS showed no net photochemistry when irradiated continuously, or upon repeated laser excitation. The importance of an oxidant to the net photochemistry is illustrated by the observation that solutions equilibrated with 1 atm P_{O_2} gave quantum yields $\sim 5 \times$ that of air equilibrated solutions, in keeping with the higher $[\text{O}_2]$. RBS also undergoes net photochemistry in deoxygenated solutions when simple oxidants such as $\text{Co}(\text{NH}_3)_6^{3+}$ were added. Effects of ionic strength and pH on Φ_d proved negligible.

Electrospray mass spectroscopy was used to identify some products of the black

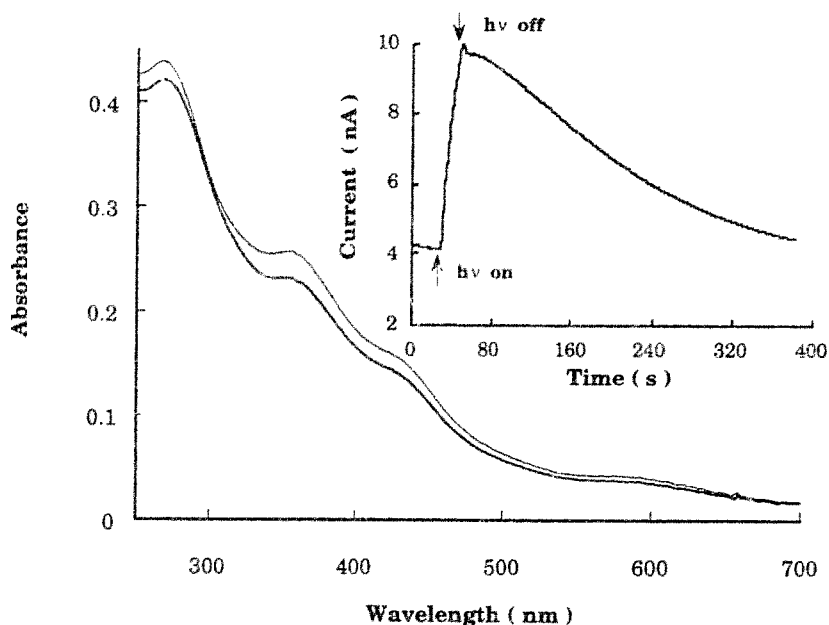


Fig. 3. Absorption changes amperogram of NO released upon white light photolysis of an aerated pH 7.0 phosphate buffered solution of Roussin's black salt. The commercial (WPI) NO sensor was used with calibrated sensitivity 0.66 nA/ μ M. Initial [RBS] = 15 μ M; Δ [RBS] from spectral changes = -1.51 μ M. Δ [NO] determined electrochemically = 9.1 μ M.

Table 1

Quantum yields for photoreactions of the Roussin's black salt $[\text{NH}_4][\text{Fe}_4\text{S}_3(\text{NO})_-]$ in various media

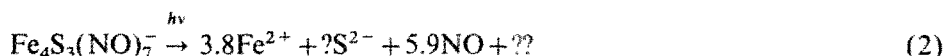
Medium	λ_{irr} (nm)	Φ_{II} (n) ^a
H ₂ O (aerobic) ^b	365	0.0011 \pm 0.0001 (10)
H ₂ O (deaerated)	365	< 10 ⁻⁶ (2)
H ₂ O (1.0 atm O ₂)	365	0.0042 (1)
H ₂ O (aerobic)	313	0.0011 \pm 0.0002 (2)
H ₂ O (aerobic)	436	0.0011 \pm 0.0002 (2)
H ₂ O (aerobic)	546	~0.001 (1)
CH ₃ OH (aerobic)	365	0.0021 \pm 0.0001 (6)
CH ₃ CN (aerobic)	365	0.0025 \pm 0.0002 (3)
THF (aerobic)	365	0.0041 \pm 0.0002 (3)

^a In moles/einstein, number of independent determinations in parentheses.

^b Unless otherwise noted all aqueous solutions are aerobic pH 7.0 phosphate buffer solution at 0.22 M ionic strength.

salt photolysis in aerated aqueous solution [22]. The RBS anion itself was well represented in the ESMS, showing both the parent at 530 m/z , as well as a series of three peaks showing losses of NO at successive -30 m/z intervals. Nitrite at 42 m/z was also a primary product, accompanied by a weak nitrate peak at 63 m/z . Signals consistent with sulfide formation were also noted in the spectrum. Solutions were

analyzed for ferrous ions by addition of 1,10-phenanthroline immediately after photolysis. This indicated nearly quantitative formation of ferrous ion [3.8 Fe(II) per RBS photolyzed]. Ferric ions were not present in significant amounts, according to analysis by thiocyanate addition. The NO released by photolysis of RBS in aerated aqueous solution was determined electrochemically as described above [16]. The moles of NO (av.) detected per mole of RBS photodecomposed equaled 5.9 ± 0.2 . Thus, the net photoreaction is a non-reversible, multi-electron process resulting in destruction of the cluster:



Roussin's red salt anion is thermally unstable in aerated solutions at neutral pH, and reacts to give RBS over the course of a few hours in the dark. When irradiated with near UV or visible light in neutral, aerated aqueous solutions, this process was markedly accelerated and gives a λ_{irr} independent quantum yield of ~ 0.14 for conversion of RRS (Table 2).

The RBS product has been identified from optical and FTIR spectra, as well as electrospray mass spectroscopy. The ESMS data also showed the formation of nitrite and sulfide. Electrochemical NO analysis in a manner analogous to that shown in Fig. 3 indicated that 0.5 mol of NO are released for each mole of RRS converted to RBS. Eq. (3) summarizes the presumed stoichiometry; the unaccounted electron

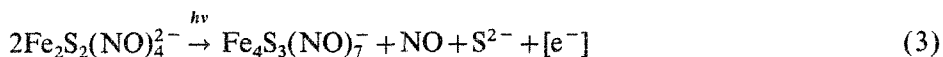
Table 2
Quantum yields for photoreactions of the Roussin's red salt $\text{Na}_3[\text{Fe}_2\text{S}_2(\text{NO})_4]$ in various media

Medium	λ_{irr} (nm)	Φ_{I}^a
H_2O^a	313	0.142 ± 0.006 (8)
H_2O (pH 7)	365	0.138 ± 0.006 (6)
H_2O (pH 7, deaerated)	365	0.0039 ± 0.0006^b (3)
H_2O (pH 6)	365	0.140 ± 0.006 (3)
H_2O (pH 8)	365	0.138 ± 0.006 (3)
H_2O (pH 9)	365	0.12 ± 0.01 (3)
H_2O (pH 10)	365	0.089 ± 0.007 (3)
H_2O	404	0.135 ± 0.006 (2)
H_2O	436	0.138 ± 0.006 (2)
H_2O	546	~ 0.13 (1)
DMSO	365	0.20 ± 0.02 (3)
MeCN	365	0.30 ± 0.02 (3)
MeCN (deaerated)	365	0.0047 ± 0.0006 (2)
Me_2CO	365	0.39 ± 0.01 (3)
MeOH	365	0.37 ± 0.01 (2)
MeOH (deaerated)	365	0.39 ± 0.01 (3)

^a In moles/einstein, number of independent determinations in parentheses.

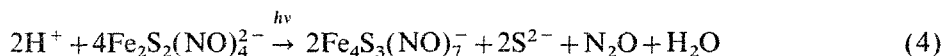
^b Unless otherwise noted all aqueous solutions are aerobic pH 7.0 phosphate buffer solution at ionic strength 0.22.

indicated by “[e[−]]” is presumed to be consumed by O₂ in these aerated solutions:

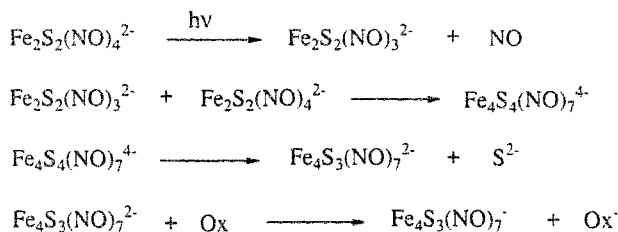


Analogous photoreaction of $\text{Fe}_2\text{S}_2(\text{NO})_4^{2-}$ also occurs in deaerated aqueous solutions, although with a much reduced Φ_d . In the absence of O₂, one must account for the extra electron. One possibility is formation of the Roussin's black salt dianion, $\text{Fe}_4\text{S}_3(\text{NO})_7^{2-}$. RBS has a series of reversible reduction potentials, the first at -0.44 V vs. NHE giving a dianionic species stable enough to be isolated [24]. The $[\text{NEt}_4]_2[\text{Fe}_4\text{S}_3(\text{NO})_7]$ salt was prepared in this laboratory by the reduction of $[\text{NEt}_4][\text{Fe}_4\text{S}_3(\text{NO})_7]$ with Zn(Hg) amalgam in the presence of excess NEt_4Br under Ar in acetonitrile. The UV-vis spectrum proved only slightly different from that of the monoanion, but the ν_{NO} bands in the FTIR spectrum shift from 1800(w), 1745(vs) and 1706(w) cm^{-1} for RBS in acetonitrile solution to 1749(m), 1690(s), 1660(sh) cm^{-1} for the dianion. Photolysis of RRS in deaerated acetonitrile under Ar clearly led to the formation of $\text{Fe}_4\text{S}_3(\text{NO})_7^{2-}$ as shown by FTIR and UV-vis spectra. However, in deoxygenated methanol or water solutions only the RBS monoanion was observed, leaving our electron count incomplete.

The only other ready target for reduction in the solution is NO itself, which has a reduction potential of -0.33 V vs. NHE. Thus, the direct reduction of NO by $\text{Fe}_4\text{S}_3(\text{NO})_7^{2-}$ is favorable ($\Delta E = +0.11$ V). This would lead to the nitroxyl anion, NO^- , which undergoes protonation, followed by the formation of nitrous oxide in protic solvents ($2\text{NO}^- + 2\text{H}^+ \rightarrow \text{H}_2\text{O} + \text{N}_2\text{O}$). Accordingly, the formation of N_2O was examined by gas chromatography of the gas phase products of the long term photolysis of a concentrated aqueous solution of RRS in a sealed cell under argon. The N_2O found was quantified, and the $\Delta\text{N}_2\text{O}/\Delta\text{RBS}$ ratio was determined as 0.5 ± 0.03 . This gives the following stoichiometry in deaerated protic solvents:



The observation of $\text{Fe}_4\text{S}_3(\text{NO})_7^{2-}$ as the photolysis product in aprotic solvents suggests a sequence of reactions such as illustrated by Scheme 1. Under conditions where other oxidants are present, this species is readily trapped, allowing for observation of NO.



Scheme 1. Proposed mechanism for RBS photoconversion.

3.2. Flash photolysis investigations of RBS and RRS

These were carried out using both time resolved infrared (TRIR) [26] and time resolved optical (TRO) [27] detection. When solutions of RBS and of RRS were subjected to flash photolysis, TRO spectral studies clearly demonstrated the presence of short lived transient species in both cases. The instability of RRS under NO prevented examination of decay rates as functions of [NO], although preliminary studies demonstrated that 355 nm flash photolysis gave transients which disappear on stepwise pathways, the rates of which were accelerated by O₂. Attempts to examine the TRIR spectra of these intermediates in non-aqueous solvents have so far proved frustrating.

The RBS system was better behaved and has been the subject of most of the studies to date. With the black salt, transient species were observed by TRO, by TRIR and by low temperature IR detection. For example, when a RBS solution in aerated tetrahydrofuran is photolyzed (365 nm) at ambient temperature, the FTIR spectra demonstrate the disappearance of RBS ν_{NO} bands, with no other product nitrosyl peaks appearing, consistent with the total destruction of the cluster. However, at -78°C , photolysis of an analogous solution led not only to the disappearance of the parent RBS bands but also to the appearance of a new species with a ν_{NO} absorbance at 1722 cm^{-1} . This intermediate disappeared when the solutions were warmed to room temperature.

The same transient spectrum was observed for deaerated RBS solutions in room temperature acetonitrile upon flash photolysis ($\lambda_{\text{irr}} = 355\text{ nm}$) with TRIR detection. The second-order disappearance of the intermediate was exactly matched by the regeneration of the parent, both traces fitting well to second-order kinetics (Fig. 4). The decay rates showed no significant changes when air is introduced to the solutions,

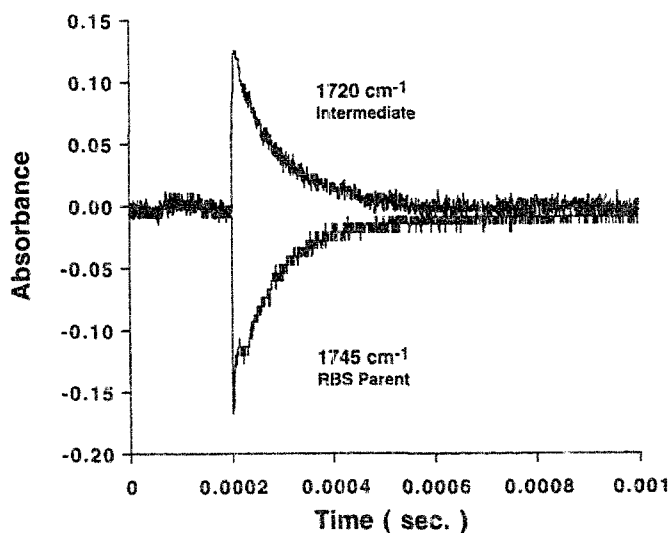


Fig. 4. Temporal IR absorbances of RBS in acetonitrile under 400 torr NO (25 °C).

but were markedly enhanced by the presence of excess NO, the kinetics now being exponential. Plots of resulting k_{obs} values vs. [NO] are linear and give the second-order rate constant $2.5 \times 10^6 \text{ M}^{-1} \text{ s}^{-1}$.

Monitoring the laser flash photolysis experiment using TRO detection revealed a new component of the decay kinetics. At 560 nm, an absorbing intermediate was seen with kinetics matching the transient observed in the TRIR; however, a slower component, appearing as a weak bleach, was also apparent. At 420 nm, a strong bleach was observed that could be fitted to biexponential decay, the slower component representing the dominant absorbance changes at this wavelength. Using data from these curves under a variety of different [NO] showed that the disappearance of each intermediate is first-order dependent in [NO] ($k_{\text{NO}} = 2.3 \times 10^6 \text{ M}^{-1} \text{ s}^{-1}$, $k'_{\text{NO}} = 3.2 \times 10^5 \text{ M}^{-1} \text{ s}^{-1}$ in CH_3CN). The results were analogous for aqueous solutions ($k_{\text{NO}} = 1.5 \times 10^7 \text{ M}^{-1} \text{ s}^{-1}$, $k'_{\text{NO}} = 8.0 \times 10^5 \text{ M}^{-1} \text{ s}^{-1}$, independent of ionic strength or pH).

Thus, laser flash photolysis of RBS leads to formation of different intermediates, both of which decay by pathways first-order in [NO], only one of which is apparent by TRIR detection. One might speculate that the two transients are the result of two independent processes of the excited state, one leading to loss of a basal NO, the other to loss of apical NO, but this is just speculation. The data suggest that the black salt's low Φ_d for net photochemistry is largely the result of the back reaction between intermediates formed by NO loss, rather than low quantum yields for the primary photoprocesses. The lifetimes of the intermediates are not affected by O_2 , indicating that even in aerated acetonitrile, reaction with dioxygen remains a minor pathway compared to trapping by NO. On the other hand, RBS undergoes no net photoreaction in the absence of an oxidant, so some trapping of an intermediate by O_2 followed by secondary thermal or photochemical processes must be responsible for the eventual photodecomposition of the cluster.

3.3. Radiation sensitization using RRS

The use of these complexes to deliver NO to biological targets was the subject of collaborative studies at the Radiation Biology Branch at the National Cancer Institute in Bethesda, MD. Nitric oxide has long been known to sensitize hypoxic (oxygen deficient) cell cultures to gamma radiation damage [28,29]. The Roussin's salts were therefore used to deliver NO photochemically to hypoxic cultures of Chinese hamster V79 cells in order to probe possible effects upon the γ -radiation sensitivity of these cells.

Fig. 5 shows the logarithmic survival rate of the cell cultures when subjected to varied irradiation doses. As can be clearly observed, treatment of the cells with RRS had little effect on the survival, but simultaneous white light irradiation greatly decreased the survival fractions of the cell cultures when exposed to γ -radiation. Visible light irradiation of the RRS incubated cell cultures without γ -radiation had little effect on survival fractions. Sensitization up to 100-fold of radiation induced cell death was observed for this and other red salt concentrations.

The black salts proved to be too cytotoxic or cytostatic to be used in such

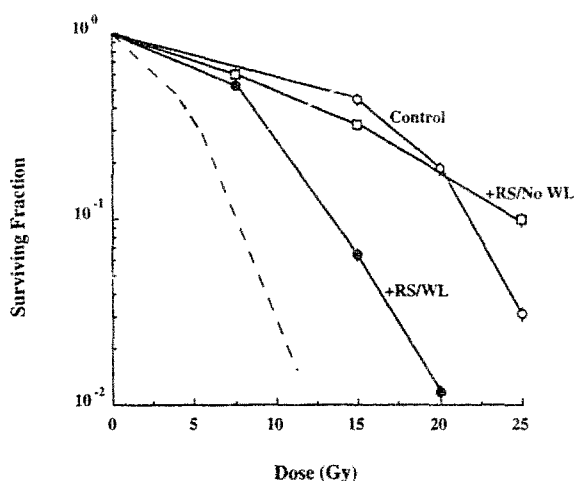


Fig. 5. Survival of V79 cells exposed to γ -radiation under hypoxic conditions in the absence (open circles) or presence of 500 μM Roussin's salt with (closed circles) or without (open squares) light exposure. The dashed line in the plot indicates the response of V79 cells exposed to γ -radiation under fully aerobic conditions (adapted from ref. [22]).

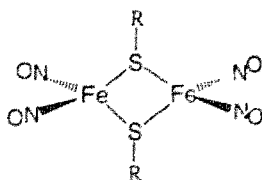
experiments, showing complete growth suppression at [RBS] as low as 200 μM . The red salt showed significant toxic effects only at concentrations of 1 mM and higher, a difference perhaps due to the greater nitrosating ability of the black salt, which is known to correlate roughly to bacteriostatic properties [30].

3.4. Roussin's red "esters"

The Roussin's red "esters" with the formula $\text{Fe}_2(\text{SR})_2(\text{NO})_4$ have so far been of limited interest in our studies, since most are insoluble in aqueous solutions. However, we have recently prepared the sulfonated derivative, $\text{Na}_2[\text{Fe}_2(\text{SCH}_2\text{CH}_2\text{SO}_3)_2(\text{NO})_4]$, and this shows both good thermal stability and high water solubility. The photolysis of this complex in aerated solutions results in the formation of 3.8 mol of NO per mole of complex photoconverted. The other products included Fe^{2+} ions and the free thiol ligands, observed by ESMS. The quantum yield for NO formation Φ_{NO} in aerated aqueous solution is ~ 0.2 , the highest value for an Fe–S–NO complex yet observed. However, these RRS esters have electronic spectra similar to that of RRS itself and do not adsorb sufficiently at longer wavelengths for in vivo studies. Efforts to improve the low energy absorption properties in this regard are underway.

4. Activation parameters for the reactions of NO with ferrihemes

The interaction of NO with hemes and other metalloporphyrin complexes has been the subject of a fruitful collaboration with Mikio Hoshino at the Institute of



Physical and Chemical Research in Japan. In particular, we have probed the kinetics of the transients formed when the nitrosyl complexes of water soluble iron(III) porphyrins $\text{Fe}^{\text{III}}(\text{P})(\text{NO})$ {where P is TPPS [tetra(4-sulfonatophenyl)porphine] or TMPS [tetra(sulfonatomesityl)porphine] or one of several proteins} were subjected to flash photolysis [31, 32]. Excitation (355 nm) of such species led to NO dissociation to give a non-steady state mixture of the nitrosyl complex $\text{Fe}(\text{P})\text{NO}$ and its solvated nitrosyl-free analog $\text{Fe}(\text{P})$. Under excess NO the transient spectra generated by flash photolysis decayed exponentially (k_{obs}) over several hundred microseconds to reform the initial equilibrium mixture of solvated and nitrosyl complexes. No permanent photoproduct was observed, thus one may conclude that the transient decay represents the relaxation of the NO system according to



If so, the rate constant observed for this first-order decay would be:

$$k_{\text{obs}} = k_{\text{on}}[\text{NO}] + k_{\text{off}} \quad (6)$$

such that a plot of k_{obs} vs. $[\text{NO}]$ would be linear with a slope k_{on} and a non-zero intercept k_{off} as illustrated in Fig. 6. Table 3 summarizes some of the k_{on} and k_{off} values measured at 25 °C for these species.

Despite the numerous flash photolysis kinetics measurements of nitric oxide reactions with various hemes, the thermal mechanisms by which NO forms and breaks bonds to the metal centers are not well characterized. The importance of this topic is not limited to the elucidation of interesting mechanisms of photochemical intermediates; it is via reactions with heme proteins such as soluble guanylyl cyclase (sGC) that NO acts as a bioregulator [34]. The concentrations of NO generated under bioregulatory conditions are quite low ($<1 \mu\text{M}$), so reaction with a desired target such as the heme iron of sGC must have very high rate constants (k_{on}) to compete effectively with other physical and chemical processes of NO depletion in the cell. To probe such pathways, we have extended earlier flash photolysis investigations of the kinetics of Eq. (5) (P=TPPS or TMPS) to a detailed mechanism examination of the “on” and “off” reactions. This involved systematic measurements of k_{on} and k_{off} as functions of the temperature (25–45 °C) (Fig. 6) and hydrostatic pressure (0.1–250 MPa) (Fig. 7) to determine ΔH^\ddagger , ΔS^\ddagger and ΔV^\ddagger for both [33]. These activation parameters [e.g. for $\text{Fe}^{\text{III}}(\text{TPPS})(\text{H}_2\text{O})_2^+$, $\Delta S_{\text{on}}^\ddagger = +86$ and $\Delta S_{\text{off}}^\ddagger = -89 \text{ J mol}^{-1} \text{ K}^{-1}$, whereas $\Delta V_{\text{on}}^\ddagger = +13$ and $\Delta V_{\text{off}}^\ddagger = +18 \text{ cm}^3 \text{ mol}^{-1}$] show a strong signature for a mechanism where the kinetically dominant steps are

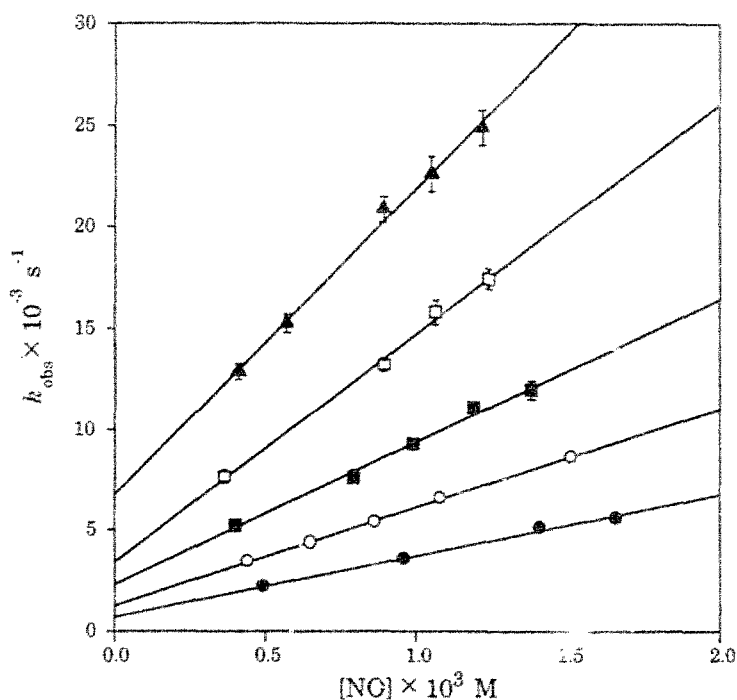
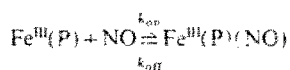


Fig. 6. Plot of k_{obs} vs. $[\text{NO}]$ at different temperatures for relaxation of the $\text{Fe}^{\text{III}}(\text{TMPS})(\text{H}_2\text{O})(\text{NO})^{2-}$ system after 355 nm flash photolysis. The slopes are k_{on} ; the intercepts are k_{off} . ● 298 K, ○ 303 K, ■ 308 K, □ 313 K, ▲ 318 K.

Table 3

Rate constants for the reaction below in 25 °C aqueous solution



Complex formed ^a	k_{on} ($\text{M}^{-1} \text{s}^{-1}$)	k_{off} (s^{-1})	$K_{\text{eq}} = k_{\text{on}} / k_{\text{off}}$ (M^{-1})
$\text{Fe}^{\text{III}}(\text{TPPS})(\text{NO})^{\text{b}}$	5.0×10^5	4.6×10^2	1.1×10^3
$\text{Fe}^{\text{III}}(\text{TMPS})(\text{NO})^{\text{b}}$	3.0×10^6	7.3×10^2	4×10^3
$\text{Mb}^{\text{III}}(\text{NO})^{\text{c}}$	1.9×10^5	13.6	1.4×10^4
$\text{Cyt}^{\text{III}}(\text{NO})^{\text{c}}$	7.2×10^2	4.4×10^{-2}	1.6×10^4
$\text{Cat}^{\text{III}}(\text{NO})^{\text{c}}$	3.0×10^7	1.7×10^2	1.8×10^5
$\text{Fe}^{\text{II}}(\text{TPPS})(\text{NO})^{\text{c}}$	1.8×10^9	~0	$> 10^9$
$\text{Mb}^{\text{II}}(\text{NO})^{\text{d}}$	1.7×10^7	1.2×10^{-4}	
$\text{Cyt}^{\text{II}}(\text{NO})^{\text{c}}$	8.3	2.9×10^{-5}	2.9×10^5

^a Mb = myoglobin, cyt = cytochrome c, cat = catalase.

^b Ref. [33].

^c Ref. [31].

^d Ref. [3].

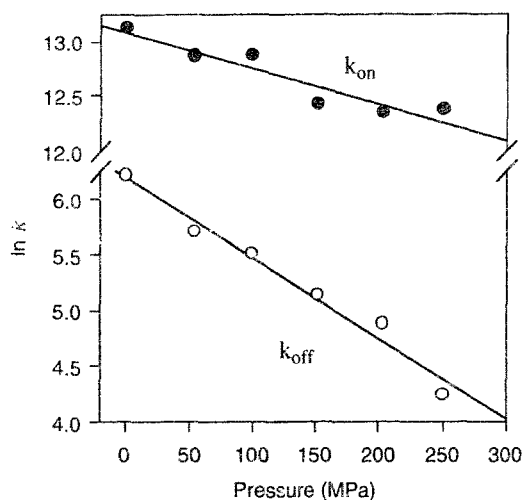


Fig. 7. Plots of $\ln k_{\text{on}}$ (●) and $\ln k_{\text{off}}$ (○) vs. hydrostatic pressure P to determine activation volume values $\Delta V_{\text{on}}^\ddagger$, $\Delta V_{\text{off}}^\ddagger$.

dissociative in character. For example, the positive ΔS^\ddagger and ΔV^\ddagger values for k_{on} are explained by a pathway where H_2O dissociation from the hexacoordinate solvento species $\text{Fe}^{\text{III}}(\text{P})(\text{H}_2\text{O})_2^{3-}$ is rate limiting as in Eqs. (7) and (8):



Consistent with this proposed mechanism is the report by Hunt and coworkers [35] that H_2O exchange between bulk solvent and $\text{Fe}^{\text{III}}(\text{TPPS})(\text{H}_2\text{O})_2^{3-}$ [Eq. (9)] occurs at a first-order rate ($k_{\text{ex}} = 1.4 \times 10^7 \text{ s}^{-1}$ in 25 °C water) exceeding the first-order relaxation rates we measured for any [NO]:



When considering the k_{off} step, it is important to recognize that formation of the nitrosyl complex is accompanied by charge transfer to give a species which can be represented as $\text{Fe}^{\text{II}}(\text{NO}^+)$ and that the metal is no longer high spin Fe(III) but, formally, low spin Fe(II). Thus, the reaction coordinate of the “off” step must incorporate entropic and volume differences related to solvation changes as charge redistributes and the system undergoes the spin cross-over accompanying NO dissociation. This may explain why $\Delta V_{\text{off}}^\ddagger > \Delta V_{\text{on}}^\ddagger$, but regardless of such speculation, the activation parameters are consistent with a dissociative mechanism in each direction.

On the larger scheme of things, the k_{on} values for Fe(II) and Fe(III) heme proteins range more than eight orders of magnitude (Table 3). The rates are very slow in cases, such as cytochrome c, where the protein limits the access of NO to the metal site, even though K values for complex formation are large. Based on

these earlier studies and the activation parameter measurements discussed here, it is clear that facile reaction of NO with metal centers requires either a very labile coordination site, as in high spin Fe^{III} heme centers such as Fe^{III}(TPPS)(H₂O)₂³⁻ and catalase ($k_{\text{on}} = 3.0 \times 10^7 \text{ M}^{-1} \text{ s}^{-1}$), or, better yet, a vacant coordination site, as in high spin Fe^{II} heme of myoglobin (1.7×10^7) and, presumably, sGC. This suggests that the free radical nature of NO, which clearly has utmost importance in determining the stability and chemical properties of biologically relevant metal nitrosyl complexes, has but minor influence on the dynamics of NO reactions to form such complexes. Since the odd electron resides in a NO π^* orbital, its involvement with the metal center is unlikely to be significant except at short distances where coordination is largely accomplished. In other words, we predict that in its “on” reactions with Fe^{II} and Fe^{III} hemes, NO acts as a normal two electron donor ligand in its initial interaction with the metal center.

5. Flash photolysis of Ru(TPP)(ONO)(NO)

In the context of developing photochemical precursors for NO delivery, it is important to build compounds which are not thermally labile. Exploratory studies in this laboratory concluded that none of the metalloporphyrin complexes of the first row transition metals gave nitrosyl complexes sufficiently substitution inert in an aerobic environment to serve such a purpose [36]. We then turned to the ruthenium analogs which are known to show a greater affinity for and lower lability of coordinated NO. Several Ru porphyrin nitrosyls were thus prepared, including the nitrosyl nitrito complex Ru(TPP)(NO)(ONO) (TPP=tetraphenylporphyrin) [37]. Described here are laser flash photolysis studies of this species in organic solvents which suggest yet a different method of NO release from a metal center.

The TRO spectrum resulting from flash photolysis of Ru(TPP)(NO)(ONO) in benzene showed the typical bleaching due to depletion of the starting material and absorptions attributed to the formation of intermediate(s) which decayed over a period of microseconds. Following the decay kinetics at a single wavelength clearly demonstrated that the temporal absorbance could be best fit to two exponentials. Fig. 8 shows the time profile for the ground state recovery, as monitored at one of the parent absorption bands. By varying [NO], it was shown that the k_{obs} values so obtained were each first order in nitric oxide. The first component's rate can be matched to a transient absorption at $\lambda_{\text{max}} = 436 \text{ nm}$, which decays under NO to give the starting material with a second-order rate constant of $2.8 \times 10^8 \text{ M}^{-1} \text{ s}^{-1}$. Another transient at $\lambda_{\text{max}} = 396 \text{ nm}$ decays an order of magnitude more slowly with the second-order rate constant for recovery of starting material equal to $2 \times 10^7 \text{ M}^{-1} \text{ s}^{-1}$. Both intermediates appear promptly after the flash and we have concluded that these are the result of two parallel photoprocesses [B \rightarrow Ru(TPP)(NO)(ONO) and C \rightarrow Ru(TPP)(NO)(ONO)]. Further details regarding the photochemistry of various ruthenium porphyrin nitrosyls of the type Ru(P)(NO)(X) (X=ONO, Cl, or OCH₃) will be described elsewhere [38].

Scheme 2 is a proposal for the formation of these two intermediates, each by NO loss from Ru(TPP)(ONO)(NO), one by direct labilization of the Ru–NO bond,

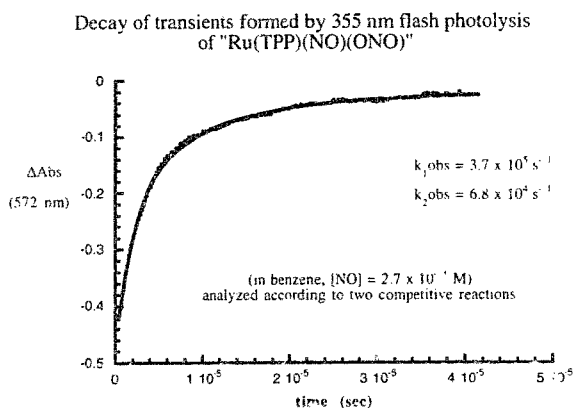
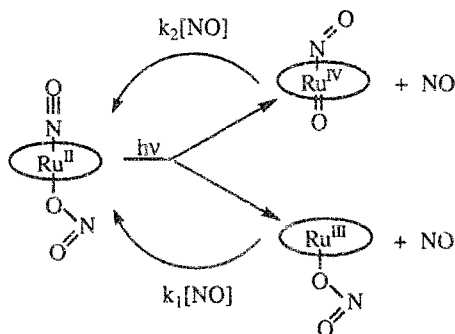


Fig. 8. Decay of transients formed by laser flash photolysis of Ru(TPP)(NO)(ONO) in benzene solution as monitored in the Q band region.

the other by cleavage of an C–NO bond in the nitrito ligand. Both intermediates presumably reassemble the parent complex by reaction with NO. Several approaches will be taken toward elucidation of this mechanism. Time resolved IR studies are being carried out both here using our tunable single frequency TRIR system and at Los Alamos National Laboratory using a stepped-scan time resolved FTIR system (with collaborator J. Schoonover). Attempts to carry out the photolyses in low temperature matrices were frustrated by the low solubility of the substrates and low photoreaction efficiencies, presumably due to geminate recombination between metalloporphyrin intermediates and NO trapped in rigid solvent cages. However, preliminary flash photolysis studies with TRIR detection were carried out with the related, more soluble Ru(TmTP)(NO)(ONO) compound (TmTP = tetra-*m*-tolylporphyrin) in ambient temperature fluid solutions. The short lived intermediate either decayed too quickly to be observed on the step scan system, or its IR spectrum displayed no new bands within the range of the detection ($2000\text{--}1540\text{ cm}^{-1}$). The longer lived intermediate showed the bleaching of the parent nitrito band at 1526 cm^{-1} and the nitrosyl band at 1852 cm^{-1} . A single transient intermediate band at 1642 cm^{-1} was



Scheme 2. Proposed mechanism for the reformation of Ru(P)(NO)(ONO) by NO dependent parallel pathways after laser flash photolysis at 355 nm.

observed, assigned to a bent nitrosyl stretch, but new nitrito bands very likely would not have been observed since the solvent absorptions of cyclohexane fall within that region. The position of the new band at 1642 cm^{-1} is somewhat unexpected, since the starting complex [$\nu_{\text{NO}} = 1840\text{ cm}^{-1}$ indicating $\text{Ru}^{\text{II}}(\text{NO}^+)$ bonding] would formally be undergoing oxidation when the O–NO bond is cleaved. Thus, if the TRIR absorbance is indeed the oxo intermediate, formal configurations such as $\text{O}=\text{Ru}^{\text{IV}}(\text{NO})$ or $\text{O}=\text{Ru}^{\text{V}}(\text{NO}^-)$ might be more accurate representations than the $\text{O}=\text{Ru}^{\text{III}}(\text{NO}^+)$ species one could write as the result of homolytic O–NO cleavage.

The changes seen in the spectra of the $\text{Ru}(\text{TPP})(\text{NO})(\text{ONO})$ are unlikely to be due to simple substitution chemistry. $\text{Ru}(\text{TPP})(\text{X})(\text{Y})$ systems tend to be relatively insensitive to the nature of the sixth ligand, shifting the Soret and Q bands only a few nanometers upon substitution, while the intermediates observed in the flash study are considerably more changed. Simple loss of the nitrosyl should result in an intermediate that can reasonably be assumed to react faster with NO than the oxo species, thus the faster component will be tentatively assigned to nitrosyl ligand loss.

The formation of an oxo complex after NO loss from ONO^- is not unprecedented. The photolyses of Cr and Mn porphyrin complexes of nitrite have been argued to give metal oxo compounds and various NO_x species [39,40]. The O–N cleavage proposed in the Ru system is homolytic, which has also been reported for these other systems. The release of NO from nitrito groups obviously suggests the use of other such systems for the delivery of NO to targets. Of special interest would be nitrito complexes with strongly oxophilic metals which may widen the scope of delivery molecules from the simpler metal nitrosyls.

6. Summary

This article has summarized recent studies in this laboratory which have been concerned with the photochemistry of metal nitrosyls. Work on the Roussin's salts has demonstrated the concept of coordination complexes as photochemical NO delivery agents to biological targets, leading to sensitization of cell to γ -radiation damage. Ongoing flash photolysis studies to elucidate mechanisms for the photochemical reactions of the black and red salts have been summarized. New complexes such as $\text{Fe}_2(\text{SCH}_2\text{CH}_2\text{SO}_3\text{Na})_2(\text{NO})_4$ hold considerable promise as more effective delivery agents, although their lack of sensitivity to red light will need to be addressed. In addition we are extending our investigations of the mechanisms of the substitution reactions of NO with ferriporphyrin and ferriheme protein systems by examining the activation parameters of the k_{on} and k_{off} rates, measured by flash photolysis kinetics. The $\text{Ru}(\text{P})(\text{ONO})(\text{NO})$ systems indicate the ability of nitrito systems to release nitric oxide and the possible formation of metal oxo species from these.

Acknowledgements

This work was supported by grants from the US National Science Foundation (CHE 9400919) and by a Collaborative UC/Los Alamos Research grant.

References

- [1] S. Moncada, R.M.J. Palmer, E.A. Higgs, *Pharmacol. Rev.* 43 (1991) 109.
- [2] M. Feelish, J.S. Stamler (Eds.), *Methods in Nitric Oxide Research*, Wiley, Chichester, UK, 1996 and references cited therein.
- [3] E.G. Moore, Q.H. Gibson, *J. Biol. Chem.* 251 (1976) 2788.
- [4] E.J. Rose, B. Hoffman, *J. Am. Chem. Soc.* 105 (1983) 2866.
- [5] M. Hoshino, S. Arai, M. Yamaji, Y. Hama, *J. Phys. Chem.* 90 (1986) 2109.
- [6] M. Hoshino, M. Kogure, *J. Phys. Chem.* 93 (1989) 5478 and references cited therein
- [7] J.W. Petrich, C. Poyart, J.L. Martin, *Biochemistry* 27 (1988) 4049.
- [8] S. Georgio, C.A. Wight, *J. Phys. Chem.* 94 (1990) 4935.
- [9] K.A. Jongeward, D. Magde, D.J. Taube, J. Marsters, T.G. Traylor, V.S. Sharma, *J. Am. Chem. Soc.* 110 (1988) 380.
- [10] T.G. Traylor, D. Magde, J. Marsters, K. Jongeward, G.-Z. Wu, K. Walda, *J. Am. Chem. Soc.* 115 (1993) 4808.
- [11] E.A. Morlino, M.A.J. Rodgers, *J. Am. Chem. Soc.* 118 (1996) 11798.
- [12] J.I. Zink, *Photochem. Photobiol.* 65 (1997) 65 and references cited therein
- [13] R.J. Singh, N. Hogg, F. Neese, J. Joseph, B. Kalyanaraman, *Photochem. Photobiol.* 61 (1995) 325.
- [14] T. Malinski, in: M. Feelish, J.S. Stamler (Eds.), *Methods in Nitric Oxide Research*, Wiley, Chichester, UK, 1996, chapter 22.
- [15] D.A. Wink, D. Christodoulou, M. Ho, M.C. Krishna, J.A. Cook, H. Haut, J.K. Randolph, M. Sullivan, G. Coia, R. Murray, T. Meyer, *Methods: A Companion to Methods in Enzymology* 7 (1995) 71.
- [16] S. Kudo, J. Bourassa, S. Boggs, Y. Sato, P.C. Ford, *Analyt. Biochem.* 247 (1997) 193.
- [17] P.C. Ford, D.A. Wink, D.M. Stanbury, *FEBS Lett.* 326 (1993) 1.
- [18] A.R. Butler, C. Glidewell, M.-H. Li, *Adv. Inorg. Chem.* 32 (1988) 335.
- [19] F.W. Flitney, I.L. Megson, J.L.M. Thomson, G.D. Kennovin, A.R. Butler, *Br. J. Pharmacol.* 117 (1996) 1549.
- [20] E.K. Matthews, E.D. Seaton, M.J. Forsyth, P.P.A. Humphrey, *Br. J. Pharmacol.* 113 (1994) 87.
- [21] T.B. Rauchfuss, T.D. Weatherill, *Inorg. Chem.* 21 (1982) 827.
- [22] J. Bourassa, W. DeGraff, S. Kudo, D.A. Wink, J.B. Mitchell, P.C. Ford, *J. Am. Chem. Soc.* 119 (1997) 2853.
- [23] S.-S. Sung, C. Glidewell, A.R. Butler, R. Hoffman, *Inorg. Chem.* 24 (1985) 3856.
- [24] S. D'Addario, F. Demartin, L. Grossi, M.C. Iapalucci, F. Laschi, G. Longoni, P. Zanello, *Inorg. Chem.* 32 (1993) 1153.
- [25] L. Noodleman, E.J. Baerends, *J. Am. Chem. Soc.* 106 (1984) 2316.
- [26] P.C. Ford, J. Bridgewater, B. Lee, *Photochem. Photobiol.* 65 (1997) 57.
- [27] E. Lindsay, P.C. Ford, *Inorg. Chim. Acta* 242 (1996) 51.
- [28] P. Howard-Flanders, *Nature (London)* 180 (1957) 1191.
- [29] J.B. Mitchell, D.A. Wink, W. DeGraff, J. Gamson, L.K. Keefer, M.C. Krishna, *Cancer Res.* 53 (1993) 5845.
- [30] X. Cui, C.L. Joannou, M.N. Hughes, R. Cammack, *FEMS Microbiol. Lett.* 98 (1992) 67.
- [31] M. Hoshino, K. Ozawa, H. Seki, P.C. Ford, *J. Am. Chem. Soc.* 115 (1993) 9568.
- [32] M. Hoshino, M. Maeda, R. Konishi, H. Seki, P.C. Ford, *J. Am. Chem. Soc.* 118 (1996) 5702.
- [33] L. Laverman, M. Hashimo, P.C. Ford, *J. Am. Chem. Soc.* 119 (1997) 12.
- [34] J.N. Burstyn, A.E. Yu, E.A. Dierks, B.K. Hawkins, J.H. Dawson, *Biochemistry* 34 (1995) 5896.
- [35] I.J. Ostrich, L. Gordon, H.W. Dodgen, J.P. Hunt, *Inorg. Chem.* 19 (1980) 619.
- [36] K. Miranda, Ph.D. Dissertation, University of California, Santa Barbara, 1996.
- [37] K. Miranda, X. Bu, I. Lorkovic, P.C. Ford, *Inorg. Chem.* 36 (1997) 4838.
- [38] I. Lorkovic, B. Lee, S. Bernhard, J. Schoonover, K. Miranda, P.C. Ford, submitted for publication.
- [39] K. Suslick, R. Watson, *Inorg. Chem.* 30 (1991) 912.
- [40] M. Yamaji, Y. Hama, M. Miyazake, M. Hoshino, *Inorg. Chem.* 31 (1992) 932.